

# Design and Development of an Embedded System for the Measurement of Boltzmann's Constant

G. Sreenivasulu and K. Raghavendra Rao\*

Department of Physics, Sri Krishnadevaraya University, Ananthapuramu - 515003, Andhra Pradesh, India;  
gummadi.sreenivasulu@gmail.com, kanchiraghavendrarao@gmail.com

## Abstract

**Objectives:** In this paper we present the design and development of an embedded system for the measurement of Boltzmann's constant using Texas Instruments' microcontroller: MSP430G2553. **Methods/ Statistical Analysis:** A transistor connected in common-base configuration with collector and base maintained at the same voltage (known as diode connected transistor or Transdiode) is used as the Device Under Test (DUT). The base-emitter voltage ( $V_{BE}$ ) is varied by a stepper motorized potentiometer whose rotation is controlled by microcontroller. The collector current ( $I_C$ ) is measured by converting it into voltage ( $V$ ) by I-to-V converter using operational amplifier. The temperature of the bath where DUT is placed is measured using LM35 temperature sensor. The base-emitter voltage  $V_{BE}$ , collector current  $I_C$  and temperature in Kelvin  $T$  are measured using MSP430G2553 microcontroller. The data is captured using terminal software PuTTY. These files are imported to the scientific graph plotting software Origin. The graphs are drawn between natural log values of  $I_C$  versus  $V_{BE}$  at ambient temperature. To perform the measurement at different temperatures a heater system with constant current source is designed and constructed in the laboratory. **Findings:** From the slope of  $\ln(I_C)$  versus  $V_{BE}$  graph Boltzmann's constant is calculated. The values of Boltzmann's constant at different temperatures are averaged and compared with standard CODATA (2014) value and percentage of error is determined. **Application/Improvement:** Microcontroller based embedded system for the measurement of Boltzmann's constant is rarely seen in literature. In the present work, a fully automatic electronic circuit for the estimation of Boltzmann's constant is designed and developed. The system is built around Texas Instruments' MSP430G2553 microcontroller and cost-effective, off-the-shelf components are used in the circuit construction.

**Keywords:** Boltzmann's Constant, Diode Connected Transistor, Energia, Embedded System, MSP430G2553 Microcontroller, PuTTY, Transdiode

## 1. Introduction

The measurement of fundamental physical constants has an important pedagogic value, because these constants determine the scale of physical phenomena<sup>1</sup>. The Boltzmann's Constant ( $k$  or  $k_B$ ) named after the *Austrian physicist Ludwig Boltzmann* is one of such physical constants which relate the energy at the individual particle level to the temperature. Boltzmann's constant is a bridge between macroscopic and microscopic physics and it is used to define the SI unit of temperature, Kelvin.

In the present method, Kelvin is defined as the fraction  $1/273.16$  of the thermodynamic temperature at the Triple Point of Water (TPW). But triple point of water

depends on many factors including pressure and precise composition of water in terms of isotopes and impurities. So this method is problematic.

In new method Kelvin is defined such that the numerical value of the Boltzmann's constant  $k$  is equal to exactly  $1.3806X \times 10^{-23} \text{ JK}^{-1}$ . Here the final "X" represents one or more digits to be determined by results of future experiments.

There are several methods to measure Boltzmann's constant, which are being performed in laboratories.

1. Acoustic method<sup>2,3</sup>
2. Spectroscopic or Doppler width of spectral lines method<sup>4-7</sup>
3. Refractive index or Dielectric constant method<sup>8</sup>

\*Author for correspondence

#### 4. Electronic method

- a) Johnson noise method<sup>9-11</sup>
- b) Transdiode or I-V Characteristic method<sup>12-14</sup>

In<sup>12</sup> the ratio of electron charge to Boltzmann's constant ( $e/k$ ) was measured using a transistor connected in Transdiode configuration. The base-emitter voltage  $V_{BE}$  and collector current  $I_C$  were measured. The slope of  $I_C$  versus  $V_{BE}$  on a semi-log graph gives  $e/kT$ . Measuring the temperature  $T$  value the ratio  $e/k$  was determined. In this method they used RCA40389 power transistor, a Hewlett-Packard model 425A current meter to measure  $I_C$  and RCA model WV-98C Senior VoltOhmist to measure  $V_{BE}$ . The measurements were made manually at three different temperatures. An error of 2% between weighted mean of measured  $e/k$  and accepted value of  $e/k$  was obtained.

In<sup>13</sup> the Boltzmann's constant was measured using TIP29 power transistor connected in Transdiode configuration. The base-emitter voltage  $V_{BE}$  was varied manually by means of a potentiometer and this voltage was measured using a digital meter. To measure the collector current  $I_C$  an op-amp IC741 was used as current-to-voltage converter. Measurements were made by changing three different feedback resistors. The graphs were drawn between logarithmic value of  $I_C$  and  $V_{BE}$  by neglecting highest values of  $I_C$  because the op-amp was saturating. The final result obtained differed by 3% of the accepted value.

In<sup>14</sup> the universal constant  $e/k$  and the energy gap of Si and Ge were measured using the forward characteristics of Si and Ge transdiodes at different temperatures in the range 150-300 K. The transdiode was mounted in a small copper cell whose bottom was soft soldered to a brass rod. The other end of the brass rod was dipped into a liquid nitrogen bath which acts as cold finger. A 30Ω constantan wire was used as heater. AD590 transducer was used as temperature sensor. LF356 operational amplifier was used as current-to-voltage converter. The forward characteristics were measured at different temperatures and semi log plots were drawn. The final value of  $e/k$  obtained was 2% less than the standard value.

5. Other methods in measuring Boltzmann's constant like studying the Brownian motion of molecules<sup>15</sup>, Atomic force microscope<sup>16</sup>, Sniffer method<sup>17</sup> and Measuring with carbon dioxide<sup>18</sup>.

In the above mentioned methods, except I-V characteristic method, other methods need expensive, sophisticated equipment and all the methods require constant human

intervention. The I-V characteristic method is inexpensive but it needs automation.

Embedded systems are being extensively used in monitoring and controlling various physical parameters<sup>19</sup>. Microcontroller based data acquisition and Boltzmann's constant measurement system is rarely seen in the literature. Keeping this in view point, we have designed and developed a fully automatic microcontroller-based embedded system to measure Boltzmann's constant. Hardware and software description of the present work are given in the following sections. Further, we have compared the experimentally measured value with standard CODATA (2014) value<sup>20</sup>.

## 2. Principle of Measurement

According to Shockley, the current-voltage (I-V) characteristics of an ideal diode is given by

$$I = I_0 \left( e^{\frac{eV}{kT}} - 1 \right) \quad (1)$$

Where  $I$  is the current and  $V$  is the voltage applied to the junction,  $e$  is the elementary charge,  $k$  is the Boltzmann's constant,  $T$  is the absolute temperature and  $I_0$  is the reverse saturation current.

But in practical diodes due to other effects like surface currents etc, the equation (1) is not exactly applicable. In this case the diode equation turns out to be

$$I = I_0 \left( e^{\frac{eV}{nkT}} - 1 \right) \quad (2)$$

Where  $n$  is called the ideality factor and its value can be anywhere between 1 and 2.5 depending on diode type and also bias voltage<sup>13</sup>. This value can be determined experimentally.

Thus, for measuring  $e/k$  or  $k$ , a diode is not a useful device, since the measurement of the I-V characteristic only gives  $e/nkT$  and  $n$  is not known a priori.

The ideal behavior equation (1) is well followed by transistors whose collector and base are kept at the same voltage. This configuration is commonly called *diode connected transistor* or *transdiode*<sup>12</sup>. For voltages  $V \gg kT$ , equation (1) turns out to be

$$I = I_0 \left( e^{\frac{eV}{kT}} \right) \quad (3)$$

In equation(3),  $V = V_{BE}$  (Base-Emitter voltage) and  $I = I_C$  (collector current) for a transistor, then

$$I_C = I_0 \left( e^{\frac{eV_{BE}}{kT}} \right) \quad (4)$$

Taking natural log on both sides, the equation (4) becomes,

$$\ln(I_C) = \ln(I_0) + (e/kT)V_{BE} \quad (5)$$

A graph of  $\ln(I_c)$  against  $V_{BE}$  should be linear with a slope of  $e/kT$ . Measuring the temperature value in Kelvin (T) and knowing  $e$  value the Boltzmann's constant  $k$  can be determined.

### 3. Proposed System

The proposed system is divided in to Hardware and Software descriptions.

#### 3.1 Hardware Description

The block diagram of developed hardware setup is shown in Figure 1. The block diagram consists of the following major blocks.

- ❖ Stepper motor controlled automatic variable power supply
- ❖ Heater system with constant current source
- ❖ Signal conditioning
- ❖ Data acquisition using MSP430G2553 microcontroller

##### 3.1.1 Stepper Motor Controlled Automatic Variable Power Supply

A stepper motor is a DC motor that moves in discrete steps. Stepper motors can be used in robotics, satellites, medical and other control applications due to their precise control. The stepper motors are basically three types.

- Variable Reluctance (VR) type
- Permanent Magnet (PM) type
- Hybrid type

Based on the phase winding there are two main sub-categories in stepper motors.

- Unipolar stepper motor
- Bipolar stepper motor

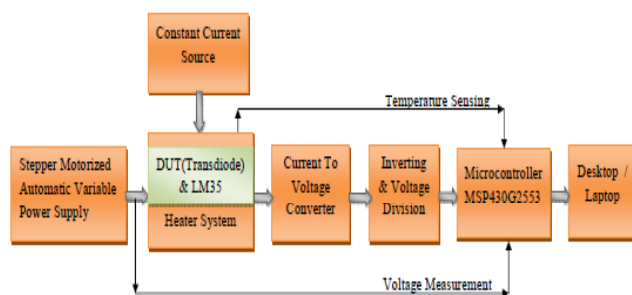


Figure 1. Block diagram of the developed system.

In the present work a hybrid type unipolar stepper motor (42BYGH036B) is used to control the variation of potentiometer. The specifications of the stepper motor are:

- Four phases
- Step angle: 1.8 degree per step
- Voltage: 12.3 V
- Current: 0.28 amp/phase
- Resistance:  $44 \pm 10\% \Omega$
- Inductance:  $21 \pm 20\% \text{ mH}$
- Holding torque: 1600 g.cm
- Detent torque: 200 g.cm

The wiper of a  $200\Omega$ , 10 turn potentiometer (Bourns, USA) is connected to the shaft of the stepper motor. The rotations of the stepper motor and hence the potentiometer is controlled by microcontroller. A DC voltage of +3.3V is connected between the potentiometer terminals. When the stepper motor rotates, the wiper of the potentiometer is rotated and variable voltage is produced. This variable voltage is applied between base and emitter of the DUT. Figure 2 shows the potentiometer coupled with the stepper motor.

To drive a stepper motor a separate driver circuit is needed because they require more power than a microcontroller can supply. In the present work ULN2003A driver circuit IC is employed to drive the stepper motor.

##### 3.1.2 Heater System and Constant Current Source

The heater system consists of an ordinary calorimeter with inner vessel containing insulating oil and an outer vessel containing water that can be cooled with ice or heated with a heating element. A  $20\Omega$  heater coil is constructed using Nichrome wire. These two vessels are kept in a wooden box with thermal insulating material. To the



Figure 2. Photograph of potentiometer coupled with the stepper motor.

cap of the calorimeter a DC motor with stirrer is attached. The DUT and LM35 temperature sensor are immersed into the insulating oil. A constant current source designed in the laboratory supplies current to the heater system. Figure 3 shows the schematic of the constant current source developed.

### 3.1.2.1 Device Under Test (DUT)

In the present paper a germanium PNP transistor AC126 and a silicon PNP transistor TIP32 connected in transdiode configuration are used as the Devices Under Test (DUT).

### 3.1.2.2 LM35 Temperature Sensor

LM35<sup>21</sup> series are precision IC temperature devices. The output voltage is linearly proportional to temperature (Celsius). They do not require any external calibration. They have linear scale factor of +10 mV/°C with ensured accuracy of 0.5°C at 25°C. LM35 is rated to operate over a -55°C to +150°C range.

### 3.1.3 Signal Conditioning

The signal conditioning circuit consists of two sections namely current-to-voltage converter and inverting amplifier & voltage division networks. In order to measure the collector current  $I_c$  with microcontroller, it is first converted into voltage employing current-to-voltage converter using operational amplifier LM356. The voltage from this section is a negative voltage. In order to measure this voltage using microcontroller it is converted in to positive voltage using another LF356 which is connected as unity gain inverting amplifier. The output voltage from this section is more than the voltage that can be applied to microcontroller (analog input of ADC). So this voltage is divided using an active voltage divider circuit using two resistors.

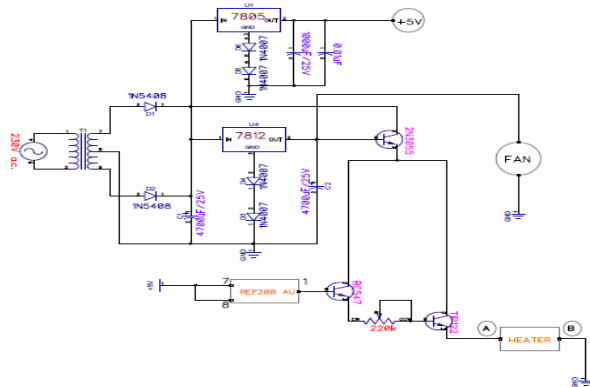


**Figure 3.** Schematic of Constant current source for the heater system.

### 3.1.3.1 LF356

LF356<sup>22</sup> is a monolithic J-FET input operational amplifier with well matched, high voltage J-FET on the same chip with standard bipolar transistors. It has low input bias and offset currents. The input offset voltage and offset voltage drifts are low. It is designed for high slew rate, wide bandwidth. It is also having an extremely fast switching time, low voltage and current noise.

### 3.1.4 MSP430G2553 Microcontroller

The microcontroller MSP430G2553<sup>23</sup> is a member of Texas instruments' mixed signal processor family. It is an ultra low power microcontroller with Von-Neumann architecture. It has five low power modes to achieve extended life. The device has a powerful 16-bit RISC Processor. The instruction set has three formats and seven addressing modes with 51 instructions. It has on-chip peripherals like two 16-bit Timers; 10-bit, 200kps Analog-to-Digital Converter; Flash memory, Hardware multiplier, Digital I/O pins, DMA controller, Comparator, USARTs, Watch Dog Timer, Brownout detector, Serial on board programming. Figure 4 shows the general architecture of MSP430G2x53 microcontroller.

The total schematic is shown in Figure 5. The power supply circuit for signal conditioning is shown in Figure 6. Figure 7 shows the photograph of the total hardware developed and interfaced with the Laptop.

### 3.2 Software Description

The software for controlling the stepper motor and for data acquisition, that is, for measuring base-emitter voltage

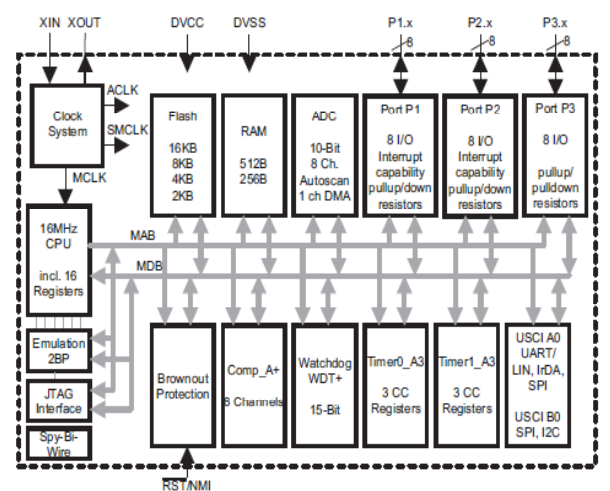


**Figure 4.** General architecture of MSP430G2x53 microcontroller.

$V_{BE}$ , collector current  $I_C$  and temperature  $T$  is developed using Energia<sup>24</sup>. The Energia is an open source electronic prototyping platform based on Arduino and the Wiring framework that includes an Integrated Development Environment (IDE) which is based on Processing<sup>25</sup>. Flow

chart of the software developed is shown in Figure 8. The screen shot of the Energia IDE is shown in Figure 9. Figure 10 shows the software program running on Energia IDE.

### 4. Methodology

A potentiometer of 200Ω and ten turn is connected to 3.3V power supply. The wiper of the potentiometer is coupled to the shaft of the stepper motor. The motion of the stepper motor is controlled by the microcontroller. When stepper motor rotates, wiper of the potentiometer turns and variable voltage is applied between base and emitter of the

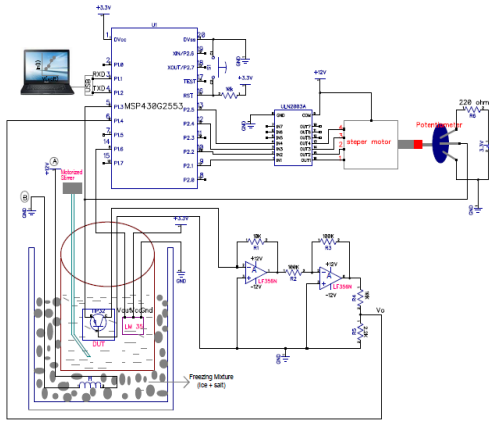


Figure 5. Total schematic of the developed system.

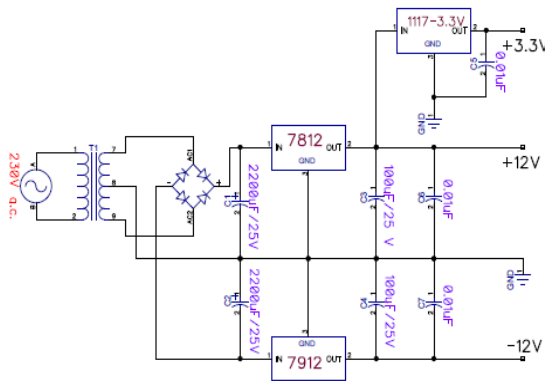


Figure 6. Schematic of Power supply for the signal conditioning circuit.

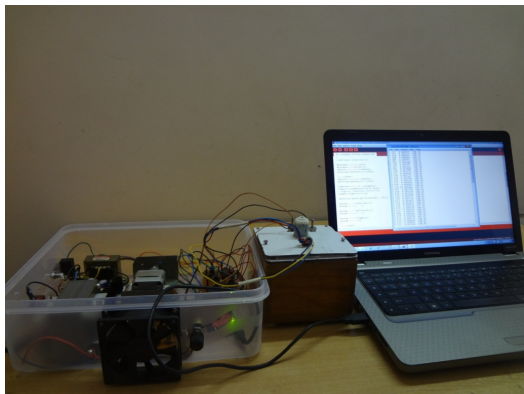


Figure 7. Photograph of the total hardware connected to the Laptop.

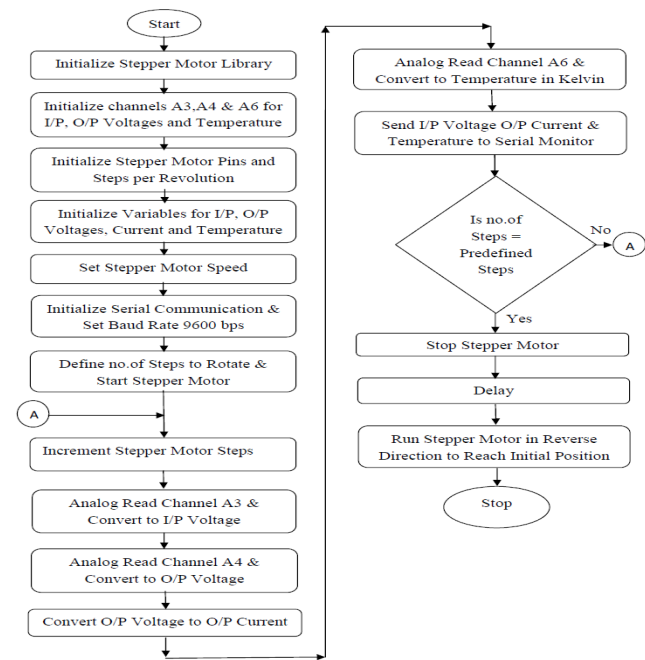


Figure 8. Flow chart of the software developed.

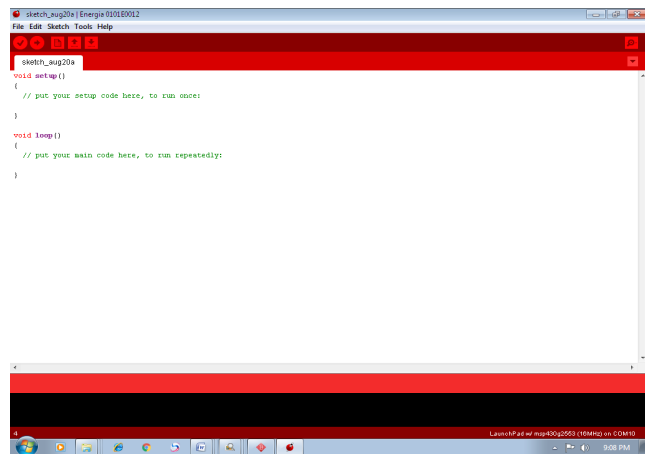


Figure 9. Screen shot of Energia IDE.

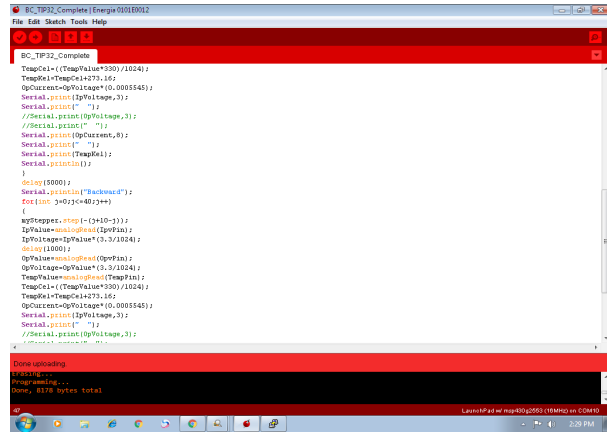


Figure 10. Screen shot of program running on Energia IDE.

DUT. This voltage  $V_{BE}$  is measured using microcontroller. The collector current  $I_C$  is applied to current-to-voltage converter LF356. The output of this op-amp is connected to another LF356 which works as unity gain inverting amplifier. The output of this op-amp is converted into current  $I_C$ . Temperature is measured using LM35 temperature sensor. To measure the voltage  $V_{BE}$ , current  $I_C$  and temperature in Kelvin  $T$ , software program is developed using Energia. The hex file is dumped on to the MSP430G2553 microcontroller. The data is captured using terminal software PuTTY<sup>26</sup>. Figure 11 shows the screen shot of the data captured by PuTTY. These files are imported to the scientific graph plotting software Origin<sup>27</sup>. The screen shot of the Origin IDE is shown in Figure 12 and data importing is shown Figure 13. The graph is drawn between  $\ln(I_C)$  and  $V_{BE}$  at ambient temperature. From slope of the linear fit of the data Boltzmann's constant is computed at that particular temperature. To perform the measurements at different temperatures DUT and LM35 are immersed in the insulating oil contained in the inner vessel of heater. Insulating oil is initially cooled down to 0°C using ice and the experiment is performed at that temperature. Now constant current is supplied to the heater and the measurements are made at different temperatures. For different constant temperatures the graphs are plotted separately at each temperature. In the present paper the experiment is carried out at five different temperatures with two types of transistors as DUTs. The mean value of Boltzmann's constant is computed and compared with the standard CODATA (2014) value  $k = 1.38064852 \times 10^{-23} \text{ J/K}$  and percentage of error is determined. To study the effect of temperature on slope of the graph, all the data are plotted on a single graph for each DUT. The experiment can

be performed without using heating system. This simplifies the experimental arrangement but the data can be obtained only at ambient temperature.

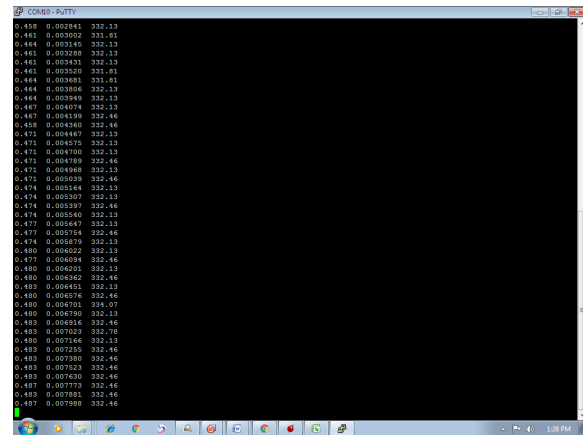


Figure 11. Screen shot of data capturing using PuTTY serial console.

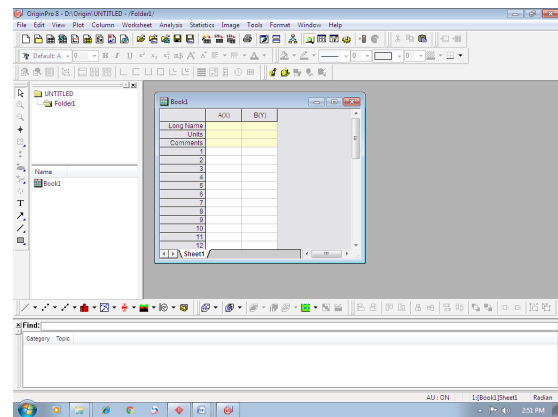


Figure 12. Screen shot of Origin graph plotting software.

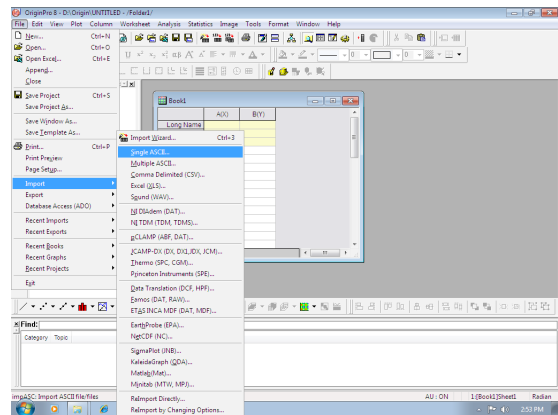


Figure 13. Screen shot of data importing to Origin.

## 5. Result and Discussion

Using AC126 and TIP32 transistors as DUTs the experiment is performed at five different temperatures. The graphs obtained for AC126 are shown in Figures 14 to 19 and the graphs for TIP32 are shown in Figures 20 to 25. The Boltzmann's constant values obtained at different temperatures are shown in Table 1 for AC126. The mean value of Boltzmann's constant is calculated and the percentage of error is determined. The measured mean value of Boltzmann's constant has an error of 1.29% of the standard CODATA (2014) value. Table 2 shows the measured Boltzmann's constant values at different temperatures for TIP32. The percentage of error in measurement in this case is 1.19%. The percentage of error obtained

**Table 1.** Boltzmann's constant values at different temperatures for AC126 transistor

Temperature(K)	Slope	Boltzmann Constant(k) J/K
273	43.62347	$1.34349832 \times 10^{-23}$
293	40.34322	$1.35357338 \times 10^{-23}$
298	39.18886	$1.37006474 \times 10^{-23}$
312	37.86763	$1.35424507 \times 10^{-23}$
328	35.03332	$1.39240266 \times 10^{-23}$
Average Boltzmann Constant $k = 1.36275683 \times 10^{-23}$ J/K		

Percentage of error in measurement =  $\frac{k_{STD} - k_{EXP}}{k_{STD}} \times 100\% = 1.29\%$

Where  $k_{STD}$  = CODATA(2014) value of Boltzmann's constant =  $1.38064852 \times 10^{-23}$  J/K

$k_{EXP}$  = Average experimental value of Boltzmann's constant =  $1.36275683 \times 10^{-23}$  J/K

**Table 2.** Boltzmann's constant values at different temperatures for TIP32 transistor

Temperature(K)	Slope	Boltzmann Constant(k) J/K
273	42.71465	$1.37208332 \times 10^{-23}$
293	40.33316	$1.35391099 \times 10^{-23}$
298	40.07472	$1.33977917 \times 10^{-23}$
312	37.64909	$1.36210599 \times 10^{-23}$
332	34.58300	$1.39353934 \times 10^{-23}$
Average Boltzmann Constant $k = 1.36428376 \times 10^{-23}$ J/K		

Percentage of error in measurement =  $\frac{k_{STD} - k_{EXP}}{k_{STD}} \times 100\% = 1.19\%$

Where  $k_{STD}$  = CODATA(2014) value of Boltzmann's constant =  $1.38064852 \times 10^{-23}$  J/K

$k_{EXP}$  = Average experimental value of Boltzmann's constant =  $1.36428376 \times 10^{-23}$  J/K

in both the cases is less than 1.5% which is also less compared to the reported values in literature.

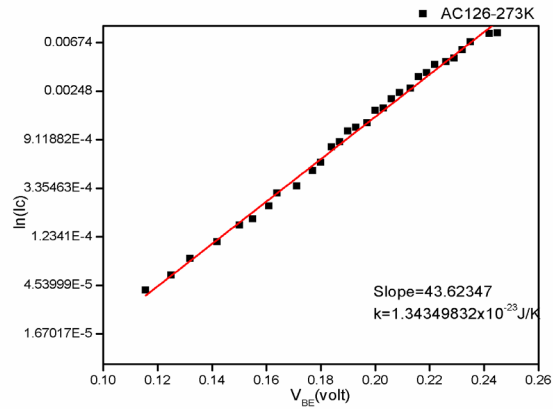


**Figure 14.** Graph of  $\ln(I_C)$  Vs  $V_{BE}$  for AC126 at 273K.

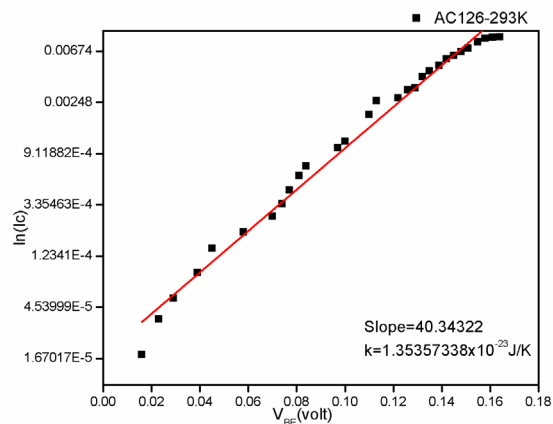


**Figure 15.** Graph of  $\ln(I_C)$  Vs  $V_{BE}$  for AC126 at 293K.

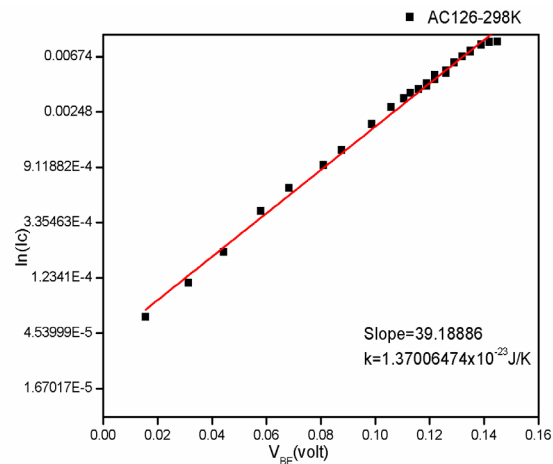


**Figure 16.** Graph of  $\ln(I_C)$  Vs  $V_{BE}$  for AC126 at 298K.

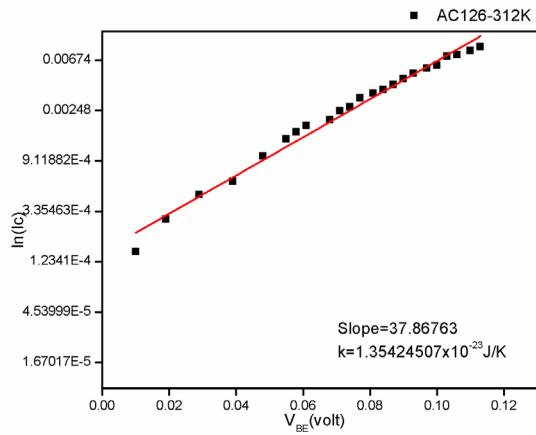


Figure 17. Graph of  $\ln(I_C)$  Vs  $V_{BE}$  for AC126 at 312K.

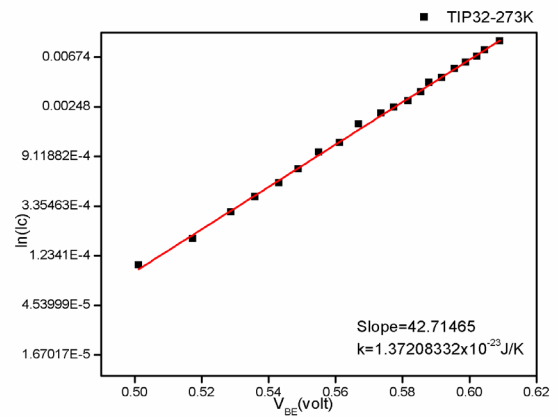


Figure 20. Graph of  $\ln(I_C)$  Vs  $V_{BE}$  for TIP32 at 273K.

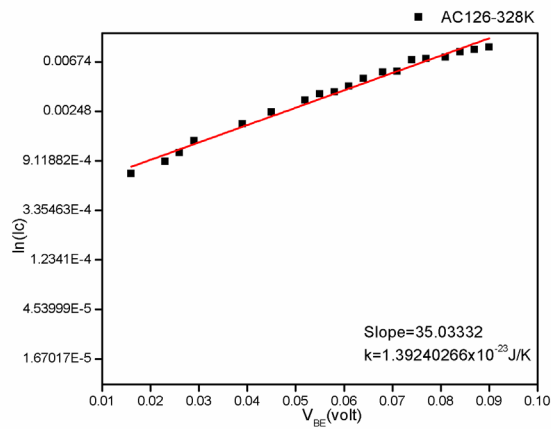


Figure 18. Graph of  $\ln(I_C)$  Vs  $V_{BE}$  for AC126 at 328K.

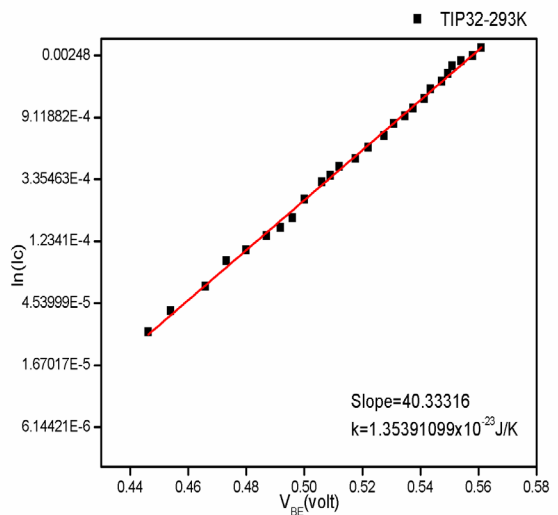


Figure 21. Graph of  $\ln(I_C)$  Vs  $V_{BE}$  for TIP32 at 293K.

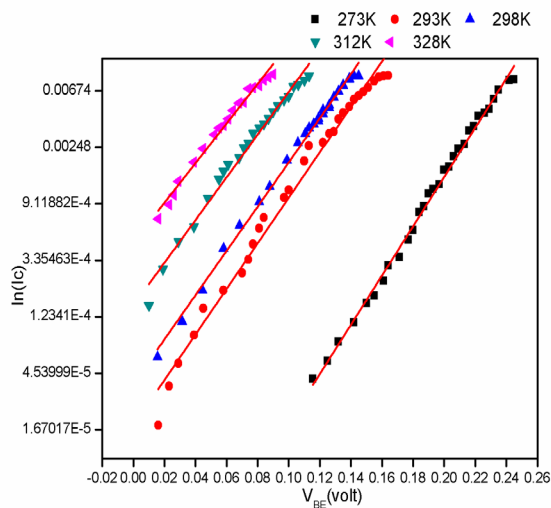


Figure 19. Graph of  $\ln(I_C)$  Vs  $V_{BE}$  for AC126 at five different temperatures.

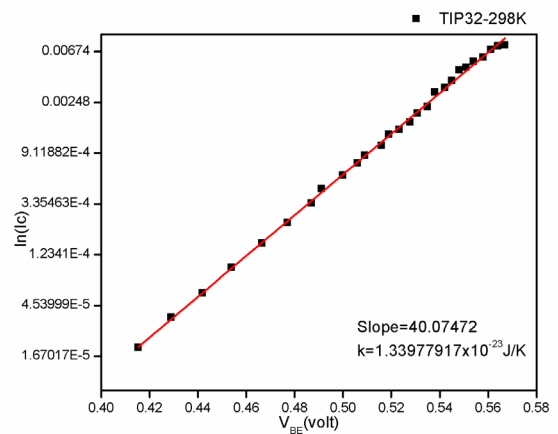


Figure 22. Graph of  $\ln(I_C)$  Vs  $V_{BE}$  for TIP32 at 298K.

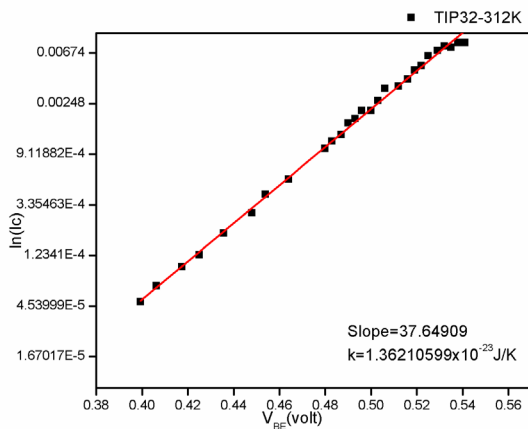


Figure 23. Graph of  $\ln(I_C)$  Vs  $V_{BE}$  for TIP32 at 312K.

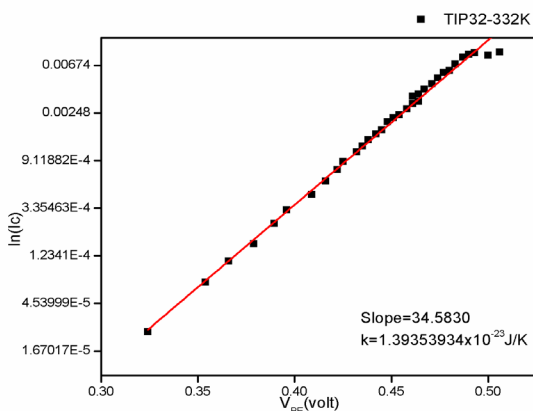


Figure 24. Graph of  $\ln(I_C)$  Vs  $V_{BE}$  for TIP32 at 332K.

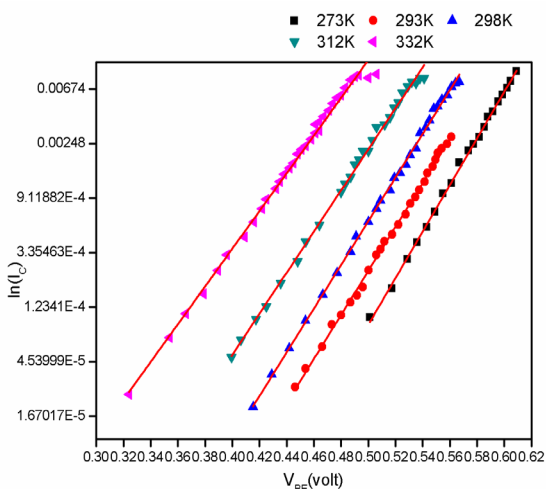


Figure 25. Graph of  $\ln(I_C)$  Vs  $V_{BE}$  for TIP32 at five different temperatures.

## 6. Conclusion

An embedded system is designed and developed for the measurement of Boltzmann's constant using MSP430G2553 microcontroller. Two transistors AC126 and TIP32 are used as DUTs. Boltzmann's constant is determined at five different temperatures for each transistor. The mean value of Boltzmann's constant measured is in good agreement with the standard CODATA (2014) value.

## 7. Acknowledgement

The authors are thankful to the Department of Science and Technology (DST), New Delhi, India for sanctioning funds under DST-FIST Program for establishing the VLSI & Embedded Systems Laboratories.

## 8. References

1. Fred W, Inmann I, Carl E, Miller M. The Measurement of  $e/k$  in the Introductory Physics Laboratory. *AJP*. 1973; 41:349–51.
2. Feng XJ, Lin H, Gillis KA, Moldover MR, Zhang JT. Test of a virtual cylindrical acoustic resonator for determining the Boltzmann constant. *Metrologia*. 2015; 52(5):343–52.
3. Pitre L, Sparasci F, Risegari L, Guianvarc'h CMD, Plimmer P, Himbert ME. Improved apparatus to determine the Boltzmann constant using a large quasi-spherical acoustic resonator. *IEEE, France*. 2014; 206–7.
4. Hald J, Nielsen L, Jan C, Petersen P. A spectroscopic determination of the Boltzmann constant. *IEEE*. 2009; 10(9):1–10.
5. Truong G W, Anstie JD, May EF, Stace TM, Luiten AN. Accurate lineshape spectroscopy and the Boltzmann constant. *Nature communications*. 2015; 6(8345):1–6.
6. Cun-Feng C, Sun YR, Shui-Ming H. Optical determination of the Boltzmann constant. *Chin Phys B*. 2015; 24(5):1–6.
7. Mejri S, Sow PLT, Kozlova O, Ayari C, Tokunaga SK, Chardonnet C, Briaudeau S, Darquie B, Rohart F, Daussy C. Measuring the Boltzmann constant by mid-infrared laser spectroscopy of ammonia. *Metrologia*. 2015; 52(1):314–23.
8. Fellmuth B, Fischer J, Gaiser C, Jusko O, Priruenrom T, Sabuga W, Zandt T. Determination of the Boltzmann constant by dielectric-constant gas thermometry. 2011; 48(5):1–23.
9. Rodriguez-Luna JC, Urquijo JD. A simple, sensitive circuit to measure Boltzmann's constant from Johnson's noise. *European Journal Physics*. 2010; 31(3):675–9.
10. Pollarolo A, Jeong T, Samuel P, Benz Rogalla BH. Johnson Noise Thermometry Measurement of the Boltzmann Constant With a 200  $\Omega$  Sense resistor. *IEEE Transactions on Instrumentation and Measurement*. 2013; 62(6):1512–7.

11. Urano C, Yamada T, Yamazawa K, Fukuyama Y, Kaneko N, Maruyama M, Domae A, Yamamori T, Yoshida S, Kiryu S. Development of Thermodynamic Temperature Measurement System Based on Quantum Voltage Noise Source at NMIJ. IEEE, Japan. 2014; 30–1.
12. Fred W, Inmann I, Carl E, Miller M. The Measurement of  $e/k$  in the Introductory Physics Laboratory. *AJP*. 1973; 41(1):349–51.
13. Evans DE. Measurement of Boltzmann's constant. *Physics Education*. 1986; 21(4):296–9.
14. Sconza A, Torzo G, Viola G. Experiment on the physics of the PN junction. *American Journal of Physics*. 1994; 62(1):66–70.
15. Nakroshis P, Amoroso M, Legere J, Smith C. Measuring Boltzmann's constant using video microscopy of Brownian motion. *Am J Phys*. 2003; 71(6):568–73.
16. Shusteff M, Burg TP, Manalis SR. Measuring Boltzmann's constant with a low-cost atomic force microscope: An undergraduate experiment. *Am J Phys*. 2006; 74(10):873–9.
17. Tyukodi B, Sarkozi ZS, Neda Z, Tunyagi A, Gyorke E. The Boltzmann constant from a sniffer. *European Journal of Physics*. 2012; 33(2):455–65.
18. Ivanov D, Nikolov S. Measuring Boltzmann's constant with carbon dioxide. *Physics education*. 2013; 48(6):713–7.
19. Sastry JKR, Ganesh JV, Bhanu JS. I<sup>2</sup>C based Networking for Implementing Heterogeneous Microcontroller based Distributed Embedded Systems. *Indian Journal of Science and Technology*. 2015 Jul; 8(15):1–10
20. Fundamental physical constants. Available from: <http://physics.nist.gov/constants>, Date accessed: 9/9/2016.
21. LF356, Wide bandwidth single J-FET operational amplifiers. Available from: <http://socrates.berkeley.edu/~phylabs/bsc/PDFFiles/LF356.pdf>, Date accessed: 15/3/2016.
22. LM35 Precision Centigrade Temperature Sensors. Available from: <http://www.ti.com/lit/ds/symlink/lm35.pdf>, Date accessed: 29/6/2016.
23. MSP430G2x53 mixed signal controller. Available from: <http://www.ti.com/lit/ds/symlink/msp430g2553.pdf>, Date accessed: 16/6/2014
24. Energia, Prototyping software to make things easy. Available from: <http://www.energia.nu/>, Date accessed: 9/3/2016
25. Gummadi S, Kanchi RR. Embedded System Laboratory Design using Texas Instruments' Launch Pad with Energia. *International Journal of Conceptions on Computing and Information Technology*. 2015; 3(1):62–8.
26. Download PuTTY. Available from: <http://www.putty.org/>, Date accessed: 15/6/2016
27. Origin lab. Available from: <http://originlab.com/>, Date accessed: 3/6/2016